J. Phys.: Condens. Matter 5 (1993) 6983–6990. Printed in the UK

On the conductivity of lateral-surface superlattices

R B S Oakeshott and A MacKinnon
Blackett Laboratory, Imperial College, London SW7 2BZ, UK

Received 1 February 1993

Abstract. We present results for the conductivity of lateral-surface superlattices with no magnetic field. For smooth potentials the results show three regimes: tunnelling between isolated states at low energies; strong scattering at intermediate energies; and weak scattering once the Fermi energy is above the top of the potential. A hard-wall potential is used to investigate the strong-scattering regime. At low energies the average conductivity is proportional to the energy, and we present a simple model which explains the average band structure in terms of the probability of reflection of a classical particle by a unit cell.

1. Introduction

Experiments on lateral-surface superlattices [1, 2] are approaching the point where effects due to interactions between the period of the lattice, the Fermi wavelength, and the magnetic length should be apparent. So far experiments on superlattices with periods of around 300 nm have shown mostly semi-classical effects [3] from the interaction of the periods of the cyclotron radius and the superlattice potential with both one-dimensional potentials [4–8] and two-dimensional potentials [9–12], although some effects have required the effect of the density of states on the scattering time to be taken into account [13–15].

For smaller periods it is hoped that purely quantum mechanical effects, seen in single systems such as point contacts [16, 17], should be apparent. In particular, a periodic potential is expected to introduce band gaps, and lower the conductivity [18].

We have recently described a technique for calculating the conductivity of lateral-surface superlattices with general potentials, and with magnetic fields [19]. We present results in this paper for systems with no magnetic field. For realistic, smooth, potentials the conductivity shows a rapid transition from strong to weak scattering as the Fermi energy rises above the maximum of the potential. Results are then shown for a hard-wall potential to investigate the strong scattering regime, where the conductivity is reduced from the conductivity with no superlattice potential. We explain the magnitude of the conductivity in terms of the average band structure estimated from the statistics of classical paths within a single unit cell.

2. Single-electron model

We adopt the simplest model for conductivity of the electrons at the interface of a GaAs/AlGaAs heterostructure, and assume a fixed periodic potential and scattering time.

0953-8984/93/376983+08$07.50

We calculate the bulk longitudinal conductivity using the formula given by Degani and Leburton [18]:

$$\sigma_{xx} = \frac{e^2\tau}{A}\sum_{k_y}\sum_{k_x}\sum_{n} v_x^2\left(-\frac{\partial f}{\partial E}\right) \tag{1}$$

where τ is the transport scattering time, v_x is the group velocity of the mode in the x direction, A is the area of the system, and f is the Fermi–Dirac distribution function. We assume in this paper a value of $\tau = 38$ ps, equivalent to a mobility of 100 $m^2\ V^{-1}\ s^{-1}$. Note that the only effect of τ within this formula is to scale the conductivity.

We have discussed in a previous paper [19] the assumptions which we are making in using this model, and shown how one can efficiently evaluate the conductivity and density of states using a recursive Green-function technique.

3. Results

Since the electrons are separated from the gates, the short-range components of the potential are damped [20] and a potential with only a few Fourier components is adequate. We therefore use a smooth potential

$$V(x, y) = \tfrac{1}{4}V_{\max}\left[\cos(2\pi x/a) + \cos(2\pi y/a) - 0.5\cos(2\pi x/a)\cos(2\pi y/a) + 2.5\right] \tag{2}$$

as considered recently by Smoliner *et al* [21]. Other smooth potentials give similar results. The amplitude of the potential can be up to of the order of 10 meV, and comparable with the Fermi energy. There are two important scales to the potential: V_{saddle} such that for Fermi energies below V_{saddle} particles are classically trapped; and the maximum height of the potential $V_{\max}$. Figure 1 shows the conductivity for different values of $V_{\max}$ for a lattice period of 100 nm. The results show a rapid transition to weak scattering as the Fermi energy is increased.

This general behaviour is what we would expect semi-classically: that is, for point particles following Newton's equation of motion between scattering events. Below V_{saddle} the conductivity is classically zero. Quantum mechanics alters the classical picture below V_{saddle} by quantizing the states in an isolated dot, which are then broadened by tunnelling to form bands. The results show however that the conductivity due to the tunnelling is small. Note that our results will not be physically accurate in this limit, since disorder will localize states in the narrow bands. For a recent review of localization effects see the book by Ulloa *et al* [22].

For large energies the potential will only weakly scatter particles within a time τ, and the conductivity will be determined by the cut-off time τ. Since $v \propto \sqrt{E - V}$ we expect

$$\sigma \propto (E - V)\,. \tag{3}$$

We have also calculated the semi-classical conductivity by evaluating $D = \langle x^2\rangle/2\tau$ for classical paths with energy E and a mean time τ, and assuming the density of states of the unperturbed electron gas. Figure 2 shows the simple estimate of equation (3), together with the quantum-mechanical and semi-classical results. The quantum-mechanical and semi-classical results for the conductivity are similar, and are given approximately by the simple estimate. The agreement between these results implies that we are looking at short times

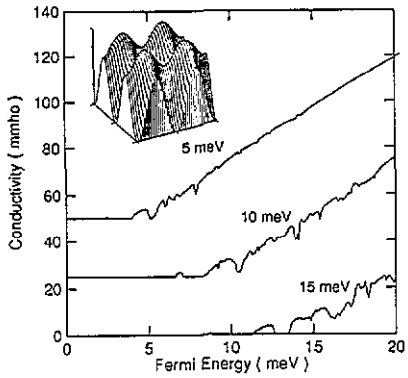

Figure 1. Conductivity for smooth potential with 100 nm lattice period and different values of peak-peak potential V_{max}. The origin of the conductivity has been shifted for clarity. The inset shows the form of the potential.

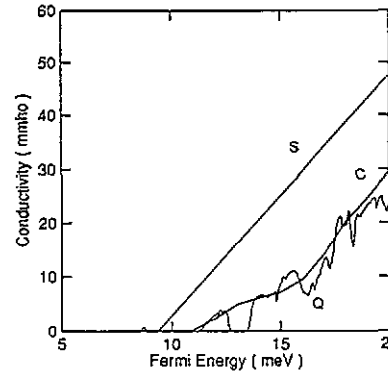

Figure 2. Comparison of conductivity for a smooth potential (curve Q) with the semi-classical conductivity (cuve C) and with a simple estimate of $\sigma = \sigma_0(1 - \langle V \rangle / E)$ (curve S). $V_{max} = 15$ meV and $a = 100$ nm. The small peak at $E_F \simeq 9$ meV is a quantum-mechanical feature: classically particles are unable to move between different unit cells at this energy.

compared with the time-scale on which the chaotic classical motion in the periodic potential produces diffusion [23], whereas the quantum-mechanical motion gives a constant group velocity. (The conductivity is smaller than equation (3) predicts because strictly we should be considering the average velocity $\langle v \rangle = \left(\int_{\text{path}} 1/v \right)^{-1}$, since the time to travel a given distance is given by the integral along the path of $1/v$. For Fermi energies above the maximum of the potential we expect the classical motion to show diffusion rather than anomalous diffusion [23] so that for large τ the conductivity is determined classically by the periodic potential, whereas quantum mechanically the conductivity increases proportionally to τ unless another scattering mechanism is introduced.)

Quantum mechanically we can understand the high-energy regime in a nearly-free-electron picture, where reflection at band edges reduces the group velocity. Within first-order perturbation theory, we expect the periodic potential to open a band-gap proportional to V_k at the band edges. Since we expect V_k to fall off with k, and since $k \propto \sqrt{E}$, so that band-gaps are more widely spaced in energy at higher energies, the conductivity will be little affected by the potential for $E_F \gg V_{max}$. Whilst some features are apparent even at relatively high energies, their size is much smaller than the amplitude of the potential.

3.1. Effect of lattice period and thermal broadening

Classically the conductivity should, neglecting any effects from the finite scattering time τ, be independent of the periodicity for a fixed potential amplitude. Quantum mechanically, as the lattice spacing is increased, the Brillouin zone becomes smaller, and the features due to interference effects are moved closer together in energy; likewise the features at a given energy correspond to higher orders in perturbation theory, and so are weaker. Figure 3 shows the conductivity for a fixed amplitude of potential, and different lattice periods displaying these features.

As the temperature is increased,the fine structure will be obscured by thermal broadening. Figure 4 shows the effect of increasing the temperature for a period of 100 nm and with $V_0 = 5$ meV.

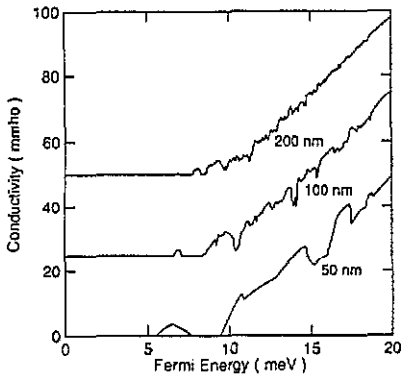

Figure 3. Conductivity for a smooth potential with 10 meV peak–peak potential and different lattice periods. The origin of the conductivity has been shifted for clarity.

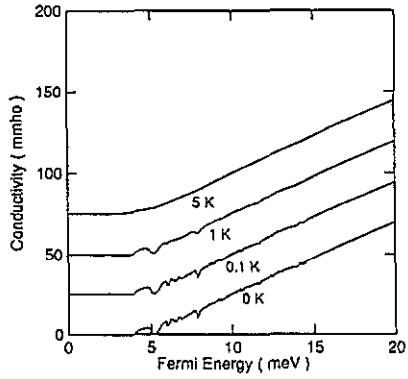

Figure 4. Conductivity for a smooth potential with 10 meV peak–peak potential and a lattice period of 100 nm for different temperatures.

4. Antidot lattice

Band effects are most apparent in the range $V_{\text{saddle}} < E < V_{\text{max}}$. We therefore also consider a hard-wall antidot potential [2], where all energies are in this range. Figure 5 shows the conductivity for an antidot lattice with the dot radius 0.25 times the lattice period. Note that the mean conductivity is smaller than with a smooth potential.

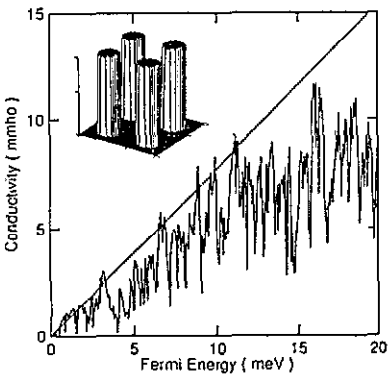

Figure 5. Conductivity for an antidot lattice with antidot radius $R_D = 0.25a$. Shown are the prediction of equation (15), (straight line); and the quantum result with $\text{Im}(E) \simeq 0$. $a = 200$ nm. The inset shows the form of the potential.

We now show how the average conductivity of the antidot lattice can be understood. The results show an initial, roughly linear portion for low energies, and a slower increase in the conductivity for higher energies. In the remainder of this section, we form an estimate of the slope for low energies from a simple path-integral picture, and argue qualitatively why the conductivity rises less rapidly at higher energies.

We have shown in a previous paper [19] how the the formula for the conductivity (equation (1)) can be written as an integral over k_y of the group velocity,

$$\sigma_{xx} \propto \int \mathrm{d}E \int \mathrm{d}k_y \sum_{\text{modes}} |v_x| \left(-\frac{\partial f}{\partial E}\right). \tag{4}$$

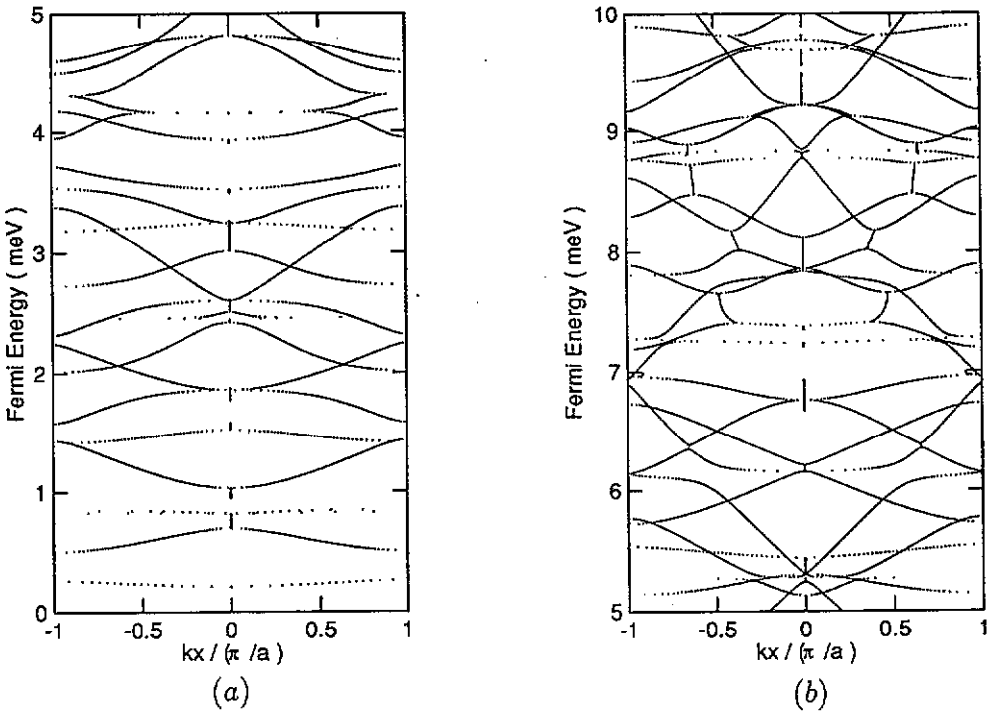

Figure 6. Band structure of an antidot lattice calculated from the eigenvalues of the transfer matrix [19] for (*a*) 0 meV $< E_F <$ 5 meV and (*b*) 5 meV $< E_F <$ 10 meV with $R_D/a = 0.25$ and $a = 200$ nm. The real part of k_x is shown for all modes with $|\log(|k/a|)| < 1$.

(The single group velocity is left after one group velocity has cancelled with a one-dimensional density of states.) Descriptions of electron transport in terms of classical paths have been used to describe transport in junctions [24–26] and to describe fluctuations in the conductivity due to quantum-mechanical interference in cavities [27–29] and we now show how the average group velocity can be found in terms of classical paths.

Let us take a single value of k_y, and form the **S** matrix for a single unit cell of the potential, with periodic boundary conditions in the y direction:

$$\begin{pmatrix} \Psi_{\text{to left on left}} \\ \Psi_{\text{to right on right}} \end{pmatrix} = \mathbf{S} \begin{pmatrix} \Psi_{\text{to right on left}} \\ \Psi_{\text{to left on right}} \end{pmatrix} \tag{5}$$

where $\Psi_{\text{to right on right}}$ etc represent the complete set of waves travelling in the directions indicated. To estimate the conductivity, we need to find the eigenvalues of the corresponding transfer matrix **T** such that

$$\begin{pmatrix} \Psi_{\text{to right on right}} \\ \Psi_{\text{to left on right}} \end{pmatrix} = \mathbf{T} \begin{pmatrix} \Psi_{\text{to right on left}} \\ \Psi_{\text{to left on left}} \end{pmatrix}. \tag{6}$$

The simplest situation, which suffices to form an estimate for low energies, is to assume that there is just a single propagating mode, and that we can neglect interactions with states almost localized in one cell, and other propagating modes. The band structure in figure 6 confirms that there is little interaction between propagating modes for low energies, but shows strong interactions between modes at higher energies.

The **S** matrix for a single mode has the general form

$$\mathbf{S} = \begin{pmatrix} it & r \\ r & it \end{pmatrix} \exp(i\phi) \tag{7}$$

where t, r, and ϕ can be chosen to be real, because of the unitarity condition $\mathbf{S}\mathbf{S}^\dagger = \mathbf{1}$, and the symmetry of the unit cell which allows us to choose the phases of the two diagonal elements to be equal without loss of generality. We obtain an estimate of the parameters of this **S** matrix by considering all the classical paths starting on face A, and ending on either face A or B; in the perpendicular direction we impose periodic boundary conditions with paths crossing the boundary being assigned an extra phase $\exp(ik_y)$. The wave function leaving the cell is approximated by

$$\psi \propto \sum_{\text{paths}} \exp\left(ikl_{\text{path}} + \Phi_{\text{path}}\right) \tag{8}$$

where l_{path} is the length of the path, k is the wavenumber at the given energy, and Φ includes the contribution to the phase from the Maslov indices [30] and from the phase associated with k_y. A more formal estimate of the **S** matrix along the lines of the formalism described by Jalabert *et al* [27] would consider the paths weighted by the wavefunction of the mode considered. A simple average of all paths has however been successful in describing fluctuations in cavities [27], and we use it here for simplicity. For higher Fermi energies, where there are many different modes to consider, the approximation of considering a single mode in the **S** matrix is inappropriate anyway.

If f_{AB} is the fraction of paths which start on face A and leave by face B, and $f_{AA} = 1 - f_{AB}$ the fraction of paths which leave by face A, then estimates for r and t are

$$\langle r^2 \rangle = 1 - \langle t^2 \rangle = f_{AA}. \tag{9}$$

Since the classical paths are independent of the Fermi energy,

$$\langle \partial t/\partial E \rangle = \langle \partial r/\partial E \rangle = 0. \tag{10}$$

In order to determine the average properties of the band structure, we do not need the absolute value of the phase ϕ, but only $\langle \partial\phi/\partial E \rangle$. The appropriate estimate is

$$\langle \partial\phi/\partial E \rangle = \langle l \rangle \, \partial k/\partial E \tag{11}$$

where $l = \langle l_{\text{path}} \rangle$. The average over paths is taken over both reflected and transmitted paths, which gives the correct answer in the limit of zero, or total reflection. The estimate is not quite trivially obvious because the phase of the reflected and transmitted waves, which one might think to be independent, are constrained by the fact that **S** must be unitary for the flux to be conserved for any combination of input waves.

Given the **S** matrix for one unit cell, we now deduce the band structure. Rearranging, we find

$$\mathbf{T} = \begin{pmatrix} 1/[t\exp(i\phi)] & ir/t \\ -ir/t & 1/[t\exp(i\phi)] \end{pmatrix} \tag{12}$$

which has eigenvalues

$$\lambda = \exp(ik_x) = \cos\phi/t \pm \sqrt{\cos^2\phi/t^2 - 1} \tag{13}$$

so that we have an estimate for the group velocity,

$$v_x = (1/\hbar)\partial E/\partial k_x = (\langle l_0\rangle / \langle l\rangle)\left(\sqrt{t^2 - \cos^2\phi/\sin\phi}\right)\sqrt{2E/m_e} \tag{14}$$

where l_0 is the average path length with no antidots present. The conductivity is then proportional to the number of open modes, multiplied by the average group velocity. The number of propagating modes is approximately the number of open modes in one of the constrictions between the antidots, which is proportional to $\sqrt{E}$, so we recover the simple result that the conductivity is proportional to the energy.

Table 1. Factors reducing group velocity in antidot lattice. The dot radius is given as a fraction of the lattice period. All other figures are relative to the empty lattice. f_{band} is the fraction of energies in a band, rather than a band gap; f_{group} is the reduction in group velocity within one band because of the opening of band gaps; and $\langle v_g\rangle$ is the average group velocity including the effect of the increased path length, and the probability a given energy is in a band gap.

Dot radius	Path length	$\langle t^2\rangle$	f_{band}	f_{group}	$\langle v_g\rangle$	σ/σ_0
0.15	1.33	0.80	0.70	0.78	0.41	0.28
0.25	1.61	0.72	0.65	0.73	0.30	0.14
0.35	2.05	0.65	0.60	0.68	0.20	0.06

We have performed this estimate numerically for the shapes described, with the results shown in table 1, and in figure 5. The conductivity is reduced relative to a system with a flat potential by a number of effects: reflection introduces band gaps, reducing the probability that a given mode is conducting by a factor f_{band}, and reducing the group velocity within a band by a factor f_{group}; the average path length between cells is increased because of paths which are scattered several times by the antidots within a unit cell, reducing the group velocity by a factor $\langle l_0\rangle / \langle l\rangle$, and the number of modes which can propagate with high probability though the narrow constrictions is reduced by a factor $1 - 2R_D/a$. Our estimate for σ is then

$$\sigma = \sigma_0 f_{\text{band}} f_{\text{group}} (1 - 2R_D/a) \langle l_0\rangle / \langle l\rangle \tag{15}$$

where σ_0 is the conductivity with no antidots present. The results show that this extremely simple estimate provides a reasonable estimate for the conductivity. For higher energies the conductivity increases less rapidly than this estimate would suggest because the independent mode assumption breaks down.

5. Summary

We have presented results for the conductivity of lateral-surface superlattices for a fixed relaxation time showing the effect of realistic potentials on the band conductivity.

For a soft potential the conductivity has a simple form with three regimes. For Fermi energies below the saddle point of the potential, where classically the electrons would be localized, the conductivity is determined by tunnelling, and we expect electron interaction

and localization effects to be important. For Fermi energies above the saddle point of the potential, but below the maximum of the potential, electrons are strongly scattered, and band structure effects are visible. At energies above the maximum of the potential, electrons are both classically and quantum mechanically only weakly scattered, little structure is visible in the conductivity, and the conductivity is close to the value with no periodic potential.

For a hard-wall potential, where the Fermi energy is always below the maximum of the potential, the conductivity is strongly reduced below the value with no superlattice potential. This reduction in conductivity is explained by a simple picture for the parameters of the band structure in terms of paths within a single unit cell.

References

[1] Weiss D, von Klitzing K, Ploog K and Weimann G 1990 *Surf. Sci.* **229** 88
[2] Weiss D, Grambow P, von Klitzing K, Menschig A and Weimann G 1991 *Appl. Phys. Lett.* **58** 2960
[3] Beenakker C W J 1989 *Phys. Rev. Lett.* **62** 2020
[4] Weiss D, von Klitzing K, Ploog K and Weimann G 1989 *Europhys. Lett.* **8** 179
[5] Gerhardts R R, Weiss D and von Klitzing K 1989 *Phys. Rev. Lett.* **62** 1173
[6] Winkler R W, Kotthaus J P and Ploog K 1989 *Phys. Rev. Lett.* **62** 1177
[7] Beton P H, Alves E S, Eaves L, Dellow M W, Henini M, Hughes O H, Beaumont S P and Wilkinson C D W 1990 *Phys. Rev.* B **42** 9229
[8] Beton P H, Main P C, Davison M, Dellow M W, Taylor R P, Alves E S, Eaves L, Beaumont S P and Wilkinson C D W 1990 *Phys. Rev.* B **42** 9689
[9] Liu C T, Tsui D C, Shayegan M, Ismail K, Antoniadis D A and Smith H I 1991 *Appl. Phys. Lett.* **58** 25
[10] Weiss D, Roukes M L, Menschig A, Grambow P, von Klitzing K and Weimann G 1991 *Phys. Rev. Lett.* **66** 2790
[11] Ensslin K and Petroff P M 1990 *Phys. Rev.* B **41** 12307
[12] Fang H and Stiles P 1990 *Phys. Rev.* B **41** 10171
[13] Zhang C and Gerhardts R R 1990 *Phys. Rev.* B **41** 12850
[14] Gerhardts R R and Zhang C 1991 *Surf. Sci.* **229** 92
[15] Vasilopoulos P and Peeters F M 1989 *Phys. Rev. Lett.* **63** 2120
[16] van Wees B J, van Houten H, Beenakker C W J, Williamson J G, Kouwenhoven L P, van der Marel D and Foxon C T 1988 *Phys. Rev. Lett.* **60** 848
[17] Wharam D A, Thornton T J, Newbury R, Pepper M, Ahmed H, Frost J E F, Hasko D G, Peacock D C, Ritchie D A and Jones G A C 1988 *J. Phys. C: Solid State Phys.* **21** L209
[18] Degani M and Leburton J P 1991 *Phys. Rev.* B **44** 10901
[19] Oakeshott R B S and MacKinnon A 1993 *J. Phys.: Condens. Matter* **5** 6971
[20] Kelly M J 1984 *J. Phys. C: Solid State Phys.* **17** L781
[21] Smoliner J, Rosskopf V, Berthold G, Gornik E, Böhm G and Weimann G 1992 *Phys. Rev.* B **45** 1915
[22] Ulloa S E, MacKinnon A, Castano E and Kirczenow G 1992 *Handbook on Semiconductors* vol 1, ed P T Landsberg (Amsterdam: North-Holland) p 863
[23] Wagenhuber J, Geisel T, Niebauer P and Obermair G 1992 *Phys. Rev.* B **45** 4372
[24] Beenakker C W J and van Houten H 1989 *Phys. Rev. Lett.* **63** 1857
[25] Roukes M L, Scherer A and van der Gaag B P 1990 *Phys. Rev. Lett.* **64** 1155
[26] Baranger H U, DiVincenzo D P, Jalabert R A and Stone A D 1991 *Phys. Rev.* B **44** 10637
[27] Jalabert R A, Baranger H U and Stone A S 1990 *Phys. Rev. Lett.* **65** 2442
[28] Oakeshott R B S and MacKinnon A 1992 *Superlatt. Microstruct.* **11** 145
[29] Marcus C M, Rimberg A J, Westervelt R M, Hopkins P F and Gossard A C 1992 *Phys. Rev. Lett.* **69** 506
[30] Gutzwiller M C 1990 *Chaos and Quantum Physics* ed M-J Giannoni *et al* (London: Elsevier)